

# The Accuracy of Density Functional Theory in the Description of Cation– $\pi$ and $\pi$ –Hydrogen Bond Interactions

Ana Rute Neves, Pedro Alexandrino Fernandes, and Maria João Ramos\*

REQUIMTE, Faculdade de Ciências do Porto, Rua do Campo Alegre S/N, 4169-007, Porto, Portugal

**ABSTRACT:** Cation– $\pi$  and  $\pi$ –hydrogen bond interactions are ubiquitous in protein folding, molecular recognition, and ligand–receptor associations. As such systems are routinely studied at the DFT level, it becomes essential to understand the underlying accuracy of the plethora of density functionals currently available for the description of these interactions. For that purpose, we carried out theoretical calculations on two small model systems (benzene–Na<sup>+</sup> and benzene–H<sub>2</sub>O) that represent a paradigm for those intermolecular interactions and systematically tested 46 density functionals against the results of high-level post-HF methods, ranging from MP2 to extrapolated CCSD(T)/CBS. A total of 13 basis sets were also tested to examine the convergence of the interaction energy with basis set size. The convergence was surprisingly fast, with deviations below 0.2 kcal/mol for double- $\zeta$  polarized basis sets with diffuse functions. Concerning functional benchmarking, the Truhlar group functionals were particularly well suited for the description of the  $\pi$ –hydrogen bond interactions. In the case of cation– $\pi$  interactions, there was not a clear correlation between accuracy and functional sophistication. Despite the large number of functionals predicting interaction energies within chemical accuracy (five for  $\pi$ –hydrogen bond and 20 for cation– $\pi$  interactions), not a single functional has shown chemical accuracy in both cases. Moreover, if we calculate the average error for these two interactions, only two density functionals resulted in an average error below 1.0 kcal/mol (M06 and HCTH, with average errors of 0.6 and 0.8 kcal/mol). The obtained results serve as a guide for future computer simulations on this kind of system.

## INTRODUCTION

Cation– $\pi$  and  $\pi$ –hydrogen bond ( $\pi$ -Hbond) interactions are noncovalent molecular interactions between an electron- $\pi$ -rich system and an adjacent cation or a hydrogen bond donor.

Cation– $\pi$  interactions between amino acids contribute significantly to protein folding, molecular recognition, and drug-receptor interactions.<sup>1</sup> They are frequently involved in key interactions at protein–protein interfaces, and they might participate in molecular recognition patterns at the active sites of enzymes or receptors rich in aromatic residues (Phe, Tyr, or Trp). In proteins, cation– $\pi$  interactions can arise between aromatic residues (Phe/Tyr/Trp) as the  $\pi$  component and positively charged amino acids (Lys, Arg, His) as the cation. Although Phe, Tyr, and Trp comprise 9% of the natural amino acids, they are substantially overrepresented at binding sites. One of the reasons for this is their capacity for establishing cation– $\pi$  interactions.<sup>2</sup> In fact, on average there is one cation– $\pi$  interaction for every 77 amino acids in the protein data bank. As a result, essentially all proteins of significant size have at least one cation– $\pi$  interaction. Over 25% of all Trp residues are involved in cation– $\pi$  interactions with Lys or Arg,<sup>2,3</sup> Arg being the most frequent cation.<sup>4</sup>

A large number of examples of protein–ligand associations in which these interactions take place have been described. For instance, the cation– $\pi$  interaction is exploited for neurotransmitter recognition throughout the nervous system, since receptors are rich in aromatic amino acids and make use of cation– $\pi$  interactions to bind their ligands, such as acetylcholine, GABA ( $\gamma$ -aminobutyric acid), and serotonin.<sup>2,4</sup> Cation– $\pi$  interactions are also responsible for the functioning and selectivity in ion channels.<sup>3</sup> The crystal structure of the K<sup>+</sup> channel shows that the mouth of the extracellular entrance is composed of the aromatic

rings of four conserved tyrosines, which enable the entrance of K<sup>+</sup> ions into the pocket.<sup>4</sup> Another example is the nucleosome remodeling factor BPTF, whose aromatic residues surround the Lys amino acids of histones, leaving no doubt that cation– $\pi$  interactions are important in this binding.<sup>2</sup>

These interactions are also present in DNA and RNA, as both purine and pyrimidine bases are electron- $\pi$ -rich systems commonly involved in the binding of cationic species (not only metal ions but also charged amino acid side chains) and also participate in hydrogen bonds with H-donor groups. Therefore, these interactions provide important contributions to the overall stability of enzyme and nucleotide molecules.

$\pi$ -Hbond interactions are weaker than the conventional hydrogen bonds but also play important roles. This type of hydrogen bond is crucial in solvation, hydrophobic interactions, molecular recognition, protein folding, neurotransmitter conformations, crystal packing, and cluster and micelle formation.<sup>5</sup> They seem to be particularly prevalent in molecules containing an indole or porphyrin moiety. Frequent  $\pi$ -Hbond donors include Tyr, Ser, Thr, Gln, or Asn residues.

In summary, cation– $\pi$  and  $\pi$ -Hbond interactions are ubiquitous in biological systems, and their importance and frequent inclusion in theoretical models led us to study how well theoretical calculations at the DFT level describe such important interactions.

Density Functional Theory (DFT) has become one of the most widespread methods for calculating a variety of molecular properties.<sup>6–8</sup> The main reason for the popularity of DFT is the inclusion of electron correlation without being as computationally

Received: March 10, 2011

Published: May 24, 2011

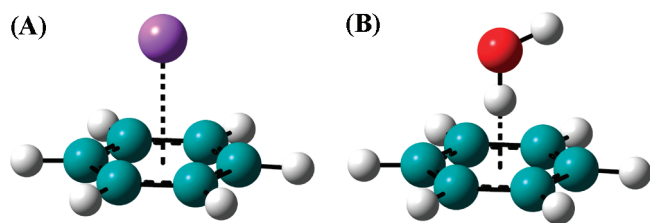


**Figure 1.** Models used in this study. (A) Benzene– $\text{Na}^+$ , which prototypically describes cation– $\pi$  interactions, and (B) benzene– $\text{H}_2\text{O}$ , which prototypically describes  $\pi$ –Hbond interactions. The dashed line represents the interatomic 6-fold symmetry axis that we have explored on the multidimensional potential energy surfaces.

demanding as other computational methods, such as post-Hartree–Fock methods. For this reason, DFT enables one to do calculations on molecules of over 100 atoms, which would be very difficult with other methods of comparable accuracy.<sup>6,9,10</sup> Today, there is a great variety of density functionals with different levels of accuracy and computational cost, and they seem to increase day after day by the desire to improve the accuracy of the DFT methodology.<sup>10</sup> For these reasons, it becomes very difficult to rate DFT functionals or to assess which one is better for a particular system or property. For readers who are interested in using DFT on systems in which cation– $\pi$  and  $\pi$ –Hbond interactions play an important role, the key question is probably which functional should be used. In the case of a lack of information, B3LYP is usually used as a default (even though this procedure is quite questionable). In fact, it is difficult to recommend any DFT functional because the number is overwhelming and each method has its own strengths and weaknesses. Therefore, it is useful to identify a small set of functionals that perform well, taking into account the properties and type of system under study, as well as the availability and computational cost associated.<sup>6,8</sup> The best way of choosing the most suitable functional for the system under study is being aware of new benchmarking studies.

Due to their importance, several studies have been devoted to evaluating the ability of DFT methods to describe nonbonded interactions.<sup>9,11–18</sup> These studies usually concentrate mostly on dispersion interactions in general terms and not individually on  $\pi$ –Hbonds and cation– $\pi$  interactions (with the exception of refs 17 and 18, which concentrate on  $\pi$ –Hbond interactions). Moreover, they analyze just a small set of density functionals and do not always address the more modern ones.

The purpose of the present article is to overcome this problem, by investigating systematically how well the plethora of current density functionals represent, in particular, cation– $\pi$  and  $\pi$ –Hbond interactions. Their correct description is essential for any reliable computer simulation in which those interactions play an important role. The obtained results serve as a guide for future computer simulations on this kind of system.

## METHODS

**I. Model Systems.** Figure 1 illustrates the two small models, benzene– $\text{Na}^+$  and benzene– $\text{H}_2\text{O}$ , on which we have carried out theoretical calculations to study cation– $\pi$  and  $\pi$ –Hbond interactions, respectively.

The model systems were specifically chosen to ensure that (i) they represented well the target biological interactions, (ii) they had a minimum number of atoms, to allow a great number of

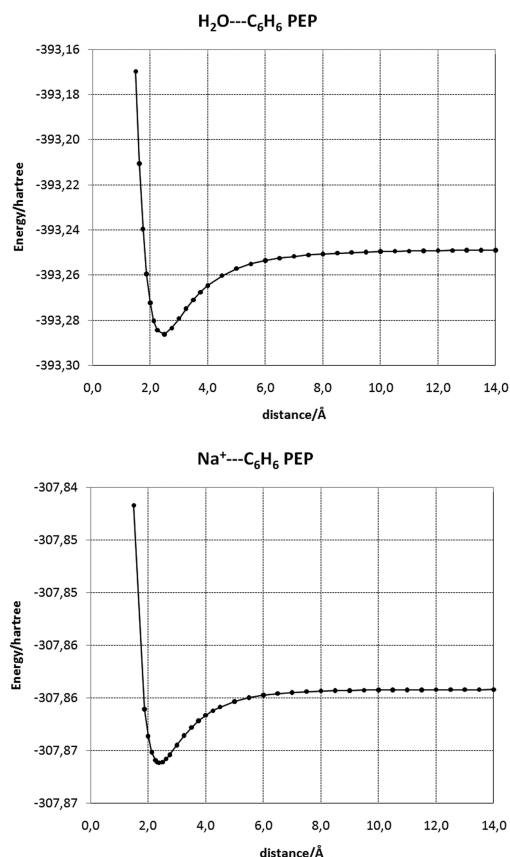


**Figure 2.** Potential energy profile along the 6-fold axis of benzene for the benzene–water system (top) and benzene–sodium ion system (bottom), calculated at the MP2/6-311++G(d,p)//MP2/6-311++G(d,p) level.

calculations and the use of computational demanding methods, such as CCSD(T) with large basis sets, (iii) they minimize the existence of other intermolecular interactions, which would otherwise complicate the interpretation of the results, and (iv) are as general as possible and not biased toward a specific system. The benzene molecule represents the  $\pi$  system. The reason for the choice of  $\text{Na}^+$  as the metal cation and  $\text{H}_2\text{O}$  molecule as the hydrogen bond donor group was that they represent well the most abundant biologically relevant Hbond/charge donors (Tyr, Ser, Thr/Arg, Lys, His, respectively), and they obey all of the exposed requisites.

**II. Potential Energy Profile.** In order to study the intermolecular interactions, we have built up a potential energy profile (PEP), by scanning different distances between the benzene molecule and the other molecular entity ( $\text{Na}^+$  or  $\text{H}_2\text{O}$ ), as shown in Figure 2 above.

These initial calculations were performed at the MP2/6-311++G(d,p) level and were carried out using the Gaussian 03 suite of programs.<sup>19</sup> The scanned coordinate was the benzene 6-fold symmetry axis. The sodium ion and one of the HO bonds of water were constrained to be along the axis. The purpose was to give a direction to the interaction that broadly mimics the one found in proteins. The PES above the benzene ring is very flat, and the water Hbond donor/cation can move very freely on the face of the ring. In biological systems, the position relative to the ring centroid is mostly determined by the protein structure and interactions. Thus, the minimum of this PEP is not rigorously a

Table 1. The DFT Functionals Tested in This Work

type	year	functional	ref.	type	year	functional	ref.
GGA	1988	BLYP	31, 32	GGE	2004	TPSSVWN5	33, 34
	1988	BP86	32, 35				
	1991	PW91PW91	36		1996	BB95	32, 37
	1992	BPW91	32, 36		1998	VSXC	38
	1996	BPBE	32, 39		2003	TPSSTPSS	33
	1996	G96LYP	31, 40		2004	PBECIS	39, 41
	1996	PBEPBE	39		2004	TPSSKCIS	33, 41
	1998	HCTH	42		2006	M06-L	9, 43
	2001	OLYP	31, 44	HM-GGA	1996	B1B95	32, 37
	2004	XLYP	31, 32, 45, 46		2003	TPSSH	33
H-GGA	1993	B3P86	35, 47		2004	BB1K	31, 32, 48
	1993	B3PW91	36, 47		2004	MPWB1K	36, 37, 48, 49
	1993	BHandH	31, 32		2004	MPW1B95	36, 37, 48, 49
	1993	BHandHLYP	31, 32		2004	MPW1KCIS	36, 41, 49, 50
	1994	B3LYP	31, 47		2004	MPWKCIS1K	36, 41, 49, 50
	1996	PBE1PBE	39		2004	mPWKCIS	36, 41, 49
	1997	B1LYP	29, 35		2005	PBE1KCIS	12, 39, 41
	1998	B97-1	42		2005	TPSS1KCIS	33, 41, 51
	1998	B98	52, 53		2005	M05	54
	2000	MPW1K	36, 49, 55		2006	M05-2X	56
	2001	B97-2	57		2006	M06-HF	9, 58
	2001	O3LYP	31, 44, 59		2008	M06-2X	9, 60
	2004	X3LYP	31, 32, 45, 46		2008	M06	9, 60
	2004	MPW3LYP	31, 36, 49				

stationary point on the free PES but is close to the structure commonly found in proteins where the residues' translational and rotational degrees of freedom are constrained by the connections to the backbone and by interactions with the remaining protein. We have also considered freely optimizing the water molecule (in which case the results would be less general and more specific for the model), but the results were almost equivalent, and the difference in energy (about 0.06 kcal/mol) was absolutely irrelevant for rating density functionals. The specific points along the 6-fold axis were chosen to give a smooth PEP with appropriate resolution near the minimum. MP2 was chosen because it provides very accurate geometries for this kind of system and because its use will not introduce any bias when comparing the density functionals, eventually favoring the functional with which the geometries were obtained, even though we must emphasize that the energy is not very sensitive to the quality of the geometry, provided that the geometry has good accuracy. At last, the two monomers were independently optimized, to provide energies at infinite separation. The different geometries along both PEPs (benzene–Na<sup>+</sup> and benzene–H<sub>2</sub>O) were then used on the following benchmarking studies.

**III. Basis Set Truncation Error.** In order to examine the convergence of the interaction energy with the completeness of the basis set, a total of 13 different basis sets were assessed, using the functional B3LYP. We have calculated single point energies for all of the points of both PEPs (benzene–Na<sup>+</sup> and benzene–H<sub>2</sub>O) and for the monomers separately. We have used the Pople basis sets 6-31G(d), 6-31+G(d), 6-31G(d,p), 6-31+G(d,p), 6-311G(d,p), 6-311+G(d,p), 6-311++G(d,p), 6-311++G(2d,2p), and 6-311++G(3df,3pd) and also the

correlation consistent basis sets cc-pVDZ, aug-cc-pVDZ, aug-cc-pVTZ, and aug-cc-pVQZ. The last one was the most complete basis set we could afford in terms of computational demand, so this was the one considered as the reference to calculate the errors on the interaction energies obtained with the other basis sets. Even so, this was not a limitation to this study, because the truncation error of the interaction energy using the aug-cc-pVQZ basis set is very low, as we will see later in the Results section. In principle, it could be possible to extrapolate the energies of the systems (and hence the interaction energy) to the complete basis set limit (CBS) using the Dunning DZ–QZ basis set series. However, the procedure to extrapolate is not well-defined within DFT, and the convergence is not necessarily consistent, contrary to what happens with wave function methods. Moreover, the results are already so close to the CBS limit that the extrapolation is not necessary here. Counterpoise (cp) corrections for basis set superposition error (BSSE) were included in the interaction energy calculations, using the Gaussian 03 software.<sup>19</sup>

**IV. Density Functional Benchmarking.** In this study, we were particularly interested in assessing the performance of DFT functionals in the description of cation– $\pi$  and  $\pi$ –Hbond intermolecular interactions. This assessment does not represent the global quality of the functionals, which must be measured through the calculation of diverse sets of properties in a representative set of molecular systems. Instead, this study just evaluates specifically the accuracy of the calculation of cation– $\pi$  and  $\pi$ –Hbond intermolecular interactions. For this purpose, we tested the performance of 46 functionals (Table 1). The extrapolated CCSD(T)/CBS energy was also obtained, with two different extrapolation methods. For the water–benzene system,



the MP2/CBS energy was calculated by the method of Truhlar using the MP2/aug-cc-pVDZ and MP2/aug-cc-pVTZ results.<sup>20</sup> Upon addition of the CCSD(T) correction (the energy difference between CCSD(T) and MP2, both with the 6-31+G(d) basis set), we obtained the extrapolated CCSD(T)/CBS energy. This procedure takes advantage of significant cancellation of the basis set truncation error in the two methods. The result was very close to other very accurate CCSD(T)/CBS extrapolations.<sup>21</sup> For Na<sup>+</sup>–benzene, we did not find other very high level calculations in the literature. This prompted us to increase even further the accuracy of our calculations. We have used a set of extrapolation techniques to obtain the extrapolated CCSD(T)/CBS energy. First, the extrapolated MP2/CBS energy was estimated using three methods: the method of Truhlar and the cc-pVXZ (X = 2–3) basis sets,<sup>22</sup> the method of Truhlar and Zhao and the aug-cc-pVXZ (X = 2–3) basis sets,<sup>20</sup> and the method of Halkier et al.<sup>23</sup> and the aug-cc-pVXZ (X = 3–4) basis sets (which constituted the highest-level extrapolation of the MP2 energy in this work). Note that in this last calculation the extrapolated HF/CBS energy was obtained with the method of Truhlar and Zhao and the aug-cc-pVXZ (X = 2–3) pair, and only the correlation energy was extrapolated with the triple and quadruple- $\zeta$  basis sets. This procedure is appropriate, as the extrapolation error is completely dominated by the correlation energy. Afterward, the energy was calculated at the CCSD(T)/aug-cc-pVTZ level, and the final extrapolated energy was obtained adding the CCSD(T) correction to the MP2 energy (i.e., the energy difference between CCSD(T) and MP2, both with the aug-cc-pVTZ basis set).

For comparison, we have also calculated the CCSD(T)/cc-pVXZ (X = 2–3) energies and used the extrapolation technique of Truhlar<sup>22</sup> with these values. All extrapolation schemes resulted in very similar interaction energies for the Na<sup>+</sup>–benzene interaction energy. The basis set superposition error (BSSE) was accounted for in the extrapolation of the MP2 energy with the method of Halkier et al. and the aug-cc-pVTZ and aug-cc-pVQZ basis sets but not with the extrapolations used with the method of Truhlar, because the last was parametrized without BSSE corrections.<sup>20,22</sup>

The choice of the density functionals was based on recent benchmarking studies,<sup>8,12,24–30</sup> which presented an overview of the current status of the field. Particular care was taken to ensure a diverse and representative choice of density functionals, including generalized gradient approximation, GGA; generalized gradient exchange, GGE; meta generalized gradient approximation, M-GGA; hybrid generalized gradient approximation, H-GGA; and hybrid meta generalized gradient approximation, HM-GGA.

The results for each density functional were obtained using single point energy calculations for selected points of the MP2/6-311++G(d,p) PEPs (benzene–Na<sup>+</sup> and benzene–H<sub>2</sub>O) and for the isolated monomers, using the 6-311++G(2d,2p) basis set. The specific distances were 1.50 Å, 1.75 Å, 2.00 Å, 2.125 Å, 2.25 Å, 2.50 Å, 2.75 Å, 3.00 Å, 3.50 Å, 4.50 Å, 5.50 Å, 6.50 Å, 8.50 Å, 10.50 Å, 12.50 Å and 14.50 Å for hydrogen–benzene centroid distances) and 2.00 Å, 2.25 Å, 2.3125 Å, 2.375 Å, 2.50 Å, 2.625 Å, 2.75 Å, 3.00 Å, 3.25 Å, 3.50 Å, 4.00 Å, 5.00 Å, 6.00 Å, 8.00 Å, 10.00 Å, 12.00 Å and 14.00 Å for sodium ions (sodium–benzene centroid distances). The distances were chosen in order to obtain a smooth PEP with appropriate resolution near the minimum. At a few points, convergence was not achieved with some hybrid-meta functionals (which are known to be numerically unstable), but these cases did not compromise at any rate

**Table 2. Electronic Interaction Energies (in kcal/mol) with ( $E_{\text{int-cp}}$ ) and without ( $E_{\text{int}}$ ) Counterpoise Correction for the Benzene–Na<sup>+</sup> Interaction and the Respective BSSEs Calculated with Several Basis Sets<sup>a</sup>**

basis set	$E_{\text{int}}$	$E_{\text{int-cp}}$	BSSE	$\Delta E_{\text{trunc}}$
6-31G(d)	–28.16	–26.11	–2.05	2.74
6-31+G(d)	–24.67	–23.58	–1.09	0.21
6-31G(d,p)	–28.06	–25.97	–2.09	2.60
6-31+G(d,p)	–24.34	–23.54	–0.80	0.17
6-311G(d,p)	–25.75	–24.53	–1.22	1.16
6-311+G(d,p)	–24.25	–23.51	–0.74	0.14
6-311++G(d,p)	–24.24	–23.51	–0.73	0.14
6-311++G(2d,2p)	–24.16	–23.45	–0.71	0.08
6-311++G(3df,3pd)	–23.90	–23.39	–0.51	0.02
cc-pVDZ	–25.06	–23.84	–1.22	0.47
aug-cc-pVDZ	–24.08	–23.55	–0.53	0.18
aug-cc-pVTZ	–23.57	–23.38	–0.19	0.01
aug-cc-pVQZ	–23.45	–23.37	–0.08	0.00

<sup>a</sup> Deviations ( $\Delta E_{\text{trunc}}$ ) between the cp-corrected interaction energies and the larger basis set (aug-cc-pVQZ) are also shown.

the correct location of the minimum and the calculation of the binding energy. The choice of the 6-311++G(2d,2p) basis set was the best compromise between the completeness of the basis set and the computational time, according to the basis set benchmarking exposed below. We have found that this basis set presented good results in describing these interaction energies, once the DFT truncation errors were probably below 0.1 kcal/mol in both systems (0.08 kcal/mol in the benzene–Na<sup>+</sup> model and 0.09 kcal/mol in the benzene–H<sub>2</sub>O model), when measured with the B3LYP functional. Moreover, this basis set is the more adequate for the benchmarking because it will be the larger that will be routinely used when dealing with large biological systems (and not model systems as the ones used here), which commonly include over 100 atoms.

The calculations with the functionals M05, M05-2X, M06, M06-2X, M06-L, M06-HF, and X3LYP were performed using the Gaussian 09 suite of programs.<sup>61</sup> All other calculations were carried out using the Gaussian 03 software package.<sup>19</sup>

The influence of the grid size used was found to be very small on the systems and properties studied here. The difference in the interaction energy calculated with the default grid (a pruned (75 302) grid) and that with the ultrafine grid (a pruned (99 590) grid) was always below 0.01 kcal/mol for the water–benzene system and below 0.1 kcal/mol for sodium–benzene system. Therefore, we have used the default grid size of both programs.

## RESULTS AND DISCUSSION

**I. Basis Set Truncation Error.** In this section, we analyze the results for the convergence of the interaction energy with basis set size. This is a quite important issue, as it directly affects the obtained accuracy and the feasibility of the calculations. DFT is known for its usual fast convergence with basis set size. In the present study, the appropriate choice of the basis set is crucial in allowing for the benchmarking of a very large number of density functionals. Tables 2 and 3 present the deviations of the interaction energies calculated for each basis set against aug-cc-pVQZ, which was the most complete one.

**Table 3.** Electronic Interaction Energies (in kcal/mol) with ( $E_{\text{int-cp}}$ ) and without ( $E_{\text{int}}$ ) Counterpoise Correction for the Benzene–H<sub>2</sub>O Interaction and the Respective BSSEs Calculated with Several Basis Sets<sup>a</sup>

basis set	$E_{\text{int}}$	$E_{\text{int-cp}}$	BSSE	$\Delta E_{\text{trunc}}$
6-31G(d)	−2.37	−1.42	−0.95	0.24
6-31+G(d)	−1.88	−1.40	−0.48	0.22
6-31G(d,p)	−2.25	−1.34	−0.91	0.16
6-31+G(d,p)	−1.71	−1.31	−0.40	0.13
6-311G(d,p)	−2.19	−1.33	−0.86	0.15
6-311+G(d,p)	−1.64	−1.30	−0.34	0.12
6-311++G(d,p)	−1.63	−1.29	−0.34	0.11
6-311++G(2d,2p)	−1.49	−1.27	−0.22	0.09
6-311++G(3df,3pd)	−1.36	−1.17	−0.19	0.01
cc-pVDZ	−2.02	−1.32	−0.70	0.14
aug-cc-pVDZ	−1.43	−1.20	−0.23	0.02
aug-cc-pVTZ	−1.26	−1.18	−0.08	0.00
aug-cc-pVQZ	−1.21	−1.18	−0.03	0.00

<sup>a</sup> Deviations ( $\Delta E_{\text{trunc}}$ ) between the cp-corrected interaction energies and the larger basis set (aug-cc-pVQZ) are also shown.

A more complete basis set is not affordable in terms of computational demand. Anyway, the result will not change significantly beyond the quadruple- $\zeta$  basis set. This can be seen in Tables 2 and 3, as increasing the complexity of the basis sets from triple- $\zeta$  (aug-cc-pVTZ) to quadruple- $\zeta$  (aug-cc-pVQZ) results in a meaningless lowering of  $E_{\text{int-cp}}$  by 0.01 kcal/mol on the benzene–Na<sup>+</sup> system and has no effect at all on the benzene–H<sub>2</sub>O system within the accuracy considered in this work. This also renders unnecessary the extrapolation to the CBS limit within DFT/B3LYP, which converges much faster than post-HF methods, for which the extrapolation is mandatory.

Considering now the remaining basis sets, one can easily isolate the three main factors that influence their accuracy: the degree of contraction of the sp shell, polarization functions, and diffuse functions.

Starting with the Pople basis sets, in the benzene–Na<sup>+</sup> system, when we move from double- $\zeta$  6-31G(d,p) to triple- $\zeta$  6-311G(d,p), the  $\Delta E_{\text{trunc}}$  decreases from 2.60 to 1.16 kcal/mol. The same happens in the benzene–H<sub>2</sub>O system, but in this case, the values are much smaller than in the benzene–Na<sup>+</sup> system (from 0.16 to 0.15 kcal/mol).

Concerning the polarization functions, in the benzene–H<sub>2</sub>O system, for example, there is a decrease in  $\Delta E_{\text{trunc}}$  from 0.11 to 0.09 kcal/mol, and then to 0.01 kcal/mol, when we move consecutively from 6-311++G(d,p) to 6-311++G(2d,2p), and to 6-311++G(3df,3pd). The polarization space seems to be saturated at this level. The same is true for the benzene–Na<sup>+</sup> system, when  $\Delta E_{\text{trunc}}$  decreases from 0.14 to 0.08 kcal/mol, and then to 0.02 kcal/mol with the same basis sets. The increase beyond the first set of polarization functions gives surprisingly small contributions to  $E_{\text{int}}$ .

We can also see that the influence of diffuse functions on heavy atoms is significant and much larger than in hydrogen atoms, as there is a decrease in  $\Delta E_{\text{trunc}}$  from 6-311G(d,p) to 6-311+G(d,p) of about 1 kcal/mol, in the benzene–Na<sup>+</sup> system, but when we add diffuse functions to hydrogen atoms (6-311++G(d,p)), the  $\Delta E_{\text{trunc}}$  remains constant. In the benzene–H<sub>2</sub>O case, we can see almost the same, but with smaller values, as has been previously said.

**Table 4.** Electronic Interaction Energies ( $E_{\text{int}}$ ), Including Counterpoise Corrections, and Their Deviation from the Reference Value ( $\Delta E_{\text{int}}$ ) in the Benzene–Na<sup>+</sup> System<sup>a</sup>

rank	functional	type	%HF	$E_{\text{int}}$	$ \Delta E_{\text{int}} $
1	mPWKCIS	M-GGA	0	−22.6	0.1
2	B3PW91	H-GGA	20	−22.8	0.1
3	BB95	M-GGA	0	−22.6	0.1
4	BLYP	GGA	0	−22.5	0.2
5	M06	HM-GGA	27	−22.9	0.2
6	HCTH	GGA	0	−22.9	0.2
7	O3LYP	H-GGA	12	−22.9	0.3
8	OLYP	GGA	0	−22.4	0.3
9	B97-2	H-GGA	21	−23.0	0.3
10	MPW1KCIS	HM-GGA	15	−23.1	0.4
11	B3P86	H-GGA	20	−23.1	0.4
12	BP86	GGA	0	−22.0	0.6
13	TPSSKCIS	M-GGA	0	−23.4	0.7
14	B3LYP	H-GGA	20	−23.4	0.8
15	TPSSTPSS	M-GGA	0	−23.6	0.9
16	BPBE	GGA	0	−21.8	0.9
17	BPW91	GGA	0	−21.7	0.9
18	B1LYP	H-GGA	25	−23.6	1.0
19	PBEKCIS	M-GGA	0	−23.7	1.0
20	TPSS1KCIS	HM-GGA	13	−23.7	1.0
21	M06-L	M-GGA	0	−21.6	1.1
22	TPSSh	HM-GGA	10	−23.8	1.1
23	TPSSVWN5	GGE	0	−21.5	1.1
24	MPWKCIS1K	HM-GGA	41	−23.9	1.2
25	B98	H-GGA	22	−24.0	1.3
26	PBE1KCIS	HM-GGA	22	−24.1	1.4
27	B1B95	HM-GGA	25	−24.2	1.5
28	PBEPBE	GGA	0	−24.3	1.6
29	B97-1	H-GGA	21	−24.4	1.7
30	MPW1K	H-GGA	43	−24.5	1.8
31	MPW3LYP	H-GGA	22	−24.5	1.8
32	X3LYP	H-GGA	21.8	−24.7	2.0
33	PW91PW91	M-GGA	0	−24.7	2.0
34	PBE1PBE	H-GGA	25	−24.8	2.1
35	BHandHLYP	H-GGA	50	−24.8	2.1
36	BB1K	HM-GGA	42	−24.9	2.2
37	G96LYP	GGA	0	−19.9	2.8
38	MPW1B95	HM-GGA	31	−25.5	2.9
39	M05	HM-GGA	28	−25.8	3.2
40	MPWB1K	HM-GGA	44	−26.0	3.3
41	M06-2X	HM-GGA	54	−26.6	4.0
42	M05-2X	HM-GGA	56	−27.2	4.5
43	BHandH	H-GGA	50	−29.8	7.1
44	VSXC	M-GGA	0	−30.9	8.2
45	M06-HF	HM-GGA	100	−31.7	9.1
46	XLYP	GGA	0	−33.1	10.4

post-HF methods	$E_{\text{int}}$
MP2/cc-pVDZ	−21.79
MP2/cc-pVTZ	−22.48
MP2/CBS <sup>b</sup>	−23.39
MP2/aug-cc-pVDZ	−21.91

Table 4. Continued

post-HF methods	$E_{\text{int}}$
MP2/aug-cc-pVTZ	−22.46
MP2/aug-cc-pVQZ	−22.66
MP2/CBS <sup>c</sup>	−23.18
MP2/CBS <sup>d</sup>	−22.74
CCSD(T)/cc-pVDZ	−21.20
CCSD(T)/cc-pVTZ	−22.34
CCSD(T)/CBS <sup>e</sup>	−23.53
CCSD(T)/aug-cc-pVDZ	−21.70
CCSD(T)/aug-cc-pVTZ	−22.40
CCSD(T)/CBS <sup>f</sup>	−23.11
CCSD(T)/CBS <sup>g</sup>	−22.67
exptl <sup>h</sup>	−20.70 ± 1.03

<sup>a</sup> All interaction energies in the table include counterpoise corrections, even though the extrapolations based on the Truhlar method were done *without* counterpoise corrections. <sup>b</sup> Extrapolated from MP2/cc-pVDZ and MP2/cc-pVTZ with the method of Truhlar.<sup>22</sup> <sup>c</sup> Extrapolated from MP2/aug-cc-pVDZ and MP2/aug-cc-pVTZ with the method of Truhlar et al.<sup>20,22</sup> <sup>d</sup> Extrapolated from MP2/aug-cc-pVTZ and MP2/aug-cc-pVQZ with the method of Halkier et al.<sup>23</sup> <sup>e</sup> Extrapolated from CCSD(T)/cc-pVDZ and CCSD(T)/cc-pVTZ with the method of Truhlar.<sup>22</sup> <sup>f</sup> Obtained adding to extrapolation 2 the CCSD(T) correction (the difference between the CCSD(T) and MP2 energies) calculated with the aug-cc-pVTZ basis set. <sup>g</sup> Obtained adding to extrapolation 3 the CCSD(T) correction (the difference between the CCSD(T) and MP2 energies) calculated with the aug-cc-pVTZ basis set. This was the most accurate calculation and was taken as a reference to rank the functionals. <sup>h</sup> Experimental value.<sup>62</sup> (Note that the ZPE energy was calculated at the MP2/6-311++G(d,p) level and subtracted from the experimental value.)

Moving on to the correlation consistent basis sets, one can say that the results are generally better than those with the Pople basis sets, as was expected. Regarding the diffuse functions, they decrease the  $\Delta E_{\text{trunc}}$  by about 0.3 kcal/mol for the benzene–Na<sup>+</sup> system and about 0.1 kcal/mol for the benzene–H<sub>2</sub>O system, when we move from the cc-pVDZ to aug-cc-pVDZ basis sets. With respect to  $\zeta$  level and polarization functions, we need to conjecture two in one, because they are inseparably within these basis sets. When we move from double- $\zeta$  (aug-cc-pVDZ) to triple- $\zeta$  (aug-cc-pVTZ), the  $\Delta E_{\text{trunc}}$  decreases considerably in benzene–Na<sup>+</sup> (approximately 0.2 kcal/mol), but the value stabilizes here, and there is no change from that point on (i.e., on moving to aug-cc-pVQZ), because we are close to the convergence limit for this property. However, in the benzene–H<sub>2</sub>O system, the increase of  $\zeta$  level and polarization functions does not influence  $\Delta E_{\text{trunc}}$  beyond the double- $\zeta$  basis. In fact, the addition of diffuse functions for the double- $\zeta$  basis set (aug-cc-pVDZ) has been enough to reduce the  $\Delta E_{\text{trunc}}$  to almost zero, giving no way to improve it.

We opted to choose the 6-311++G(2d,2p) basis set for the functional benchmarking that follows, due to the good compromise between the complexity of the basis set and the computational demand. The truncation errors associated with the use of this basis set are below 0.1 kcal/mol in both systems (0.08 kcal/mol in the benzene–Na<sup>+</sup> model and 0.09 kcal/mol in the benzene–H<sub>2</sub>O model).

It is also interesting to assess the influence of counterpoise corrections (cp) for the basis set superposition error (BSSE) in the interaction energies of both systems. The values are presented in Tables 2 and 3. The influence of the cp correction is significantly greater for the less complete basis sets, where the

Table 5. Electronic Interaction Energies ( $E_{\text{int}}$ ), Including Counterpoise Corrections, and Their Deviation from the Reference Value ( $\Delta E_{\text{int}}$ ) for the Benzene–H<sub>2</sub>O System<sup>a</sup>

rank	functional	type	%HF	$E_{\text{int}}$	$ \Delta E_{\text{int}} $
1	M06-2X	HM-GGA	54	−3.40	0.04
2	M05-2X	HM-GGA	56	−3.33	0.11
3	M06-HF	HM-GGA	100	−3.65	0.21
4	M05	HM-GGA	28	−2.58	0.86
5	BHandH	H-GGA	50	−4.37	0.93
6	M06	HM-GGA	27	−2.36	1.08
7	MPWB1K	HM-GGA	44	−2.33	1.11
8	M06-L	M-GGA	0	−2.23	1.21
9	MPW1B95	HM-GGA	31	−2.21	1.23
10	PW91PW91	M-GGA	0	−2.12	1.32
11	B97-1	H-GGA	21	−2.10	1.34
12	HCTH	GGA	0	−2.09	1.35
13	PBE1PBE	H-GGA	25	−1.95	1.49
14	PBE1KCIS	HM-GGA	22	−1.92	1.52
15	PBEPBE	GGA	0	−1.92	1.52
16	B98	H-GGA	22	−1.90	1.54
17	PBEKCIS	M-GGA	0	−1.87	1.57
18	MPW3LYP	H-GGA	22	−1.82	1.62
19	BB1K	HM-GGA	42	−1.80	1.64
20	BHandHLYP	H-GGA	50	−1.66	1.78
21	MPW1K	H-GGA	43	−1.64	1.80
22	X3LYP	H-GGA	21.8	−1.63	1.81
23	MPWKICIS1K	HM-GGA	41	−1.61	1.83
24	TPSS1KCIS	HM-GGA	13	−1.54	1.90
25	B1B95	HM-GGA	25	−1.53	1.91
26	TPSSKCIS	M-GGA	0	−1.50	1.94
27	TPSSH	HM-GGA	10	−1.46	1.98
28	MPW1KCIS	HM-GGA	15	−1.40	2.04
29	TPSSTPSS	M-GGA	0	−1.39	2.05
30	B97-2	H-GGA	21	−1.36	2.08
31	B3P86	H-GGA	20	−1.31	2.13
32	mPWKCIS	M-GGA	0	−1.28	2.16
33	B3LYP	H-GGA	20	−1.27	2.17
34	B1LYP	H-GGA	25	−1.19	2.25
35	TPSSVWN5	GGE	0	−1.12	2.32
36	BB95	M-GGA	0	−1.00	2.44
37	O3LYP	H-GGA	12	−0.98	2.46
38	B3PW91	H-GGA	20	−0.95	2.49
39	OLYP	GGA	0	−0.88	2.56
40	BP86	GGA	0	−0.82	2.62
41	BLYP	GGA	0	−0.76	2.68
42	BPW91	GGA	0	−0.59	2.85
43	BPBE	GGA	0	−0.58	2.86
44	G96LYP	GGA	0	−0.16	3.28
45	XLYP	GGA	0	−7.77	4.33
46	VSXC	M-GGA	0	−8.12	4.68
MP2/aug-cc-pVDZ				−4.52	
MP2/aug-cc-pVTZ				−3.88	
MP2/CBS <sup>b</sup>				−3.72	
MP2/6-31+G(d)				−2.16	
CCSD(T)/6-31+G(d)				−2.21	
$\Delta(\text{CCSD(T)}-\text{MP2})$				−0.05	



Table 5. Continued

MP2/aug-cc-pVDZ	−4.52
MP2/aug-cc-pVTZ	−3.88
MP2/CBS <sup>b</sup>	−3.72
MP2/6-31+G(d)	−2.16
CCSD(T)/6-31+G(d)	−2.21
$\Delta$ (CCSD(T)-MP2)	−0.05
CCSD(T)/CBS <sup>c</sup>	−3.77
exptl <sup>d</sup>	−3.44 ± 0.09

<sup>a</sup> All interaction energies in the table include counterpoise corrections, even though the extrapolations based on the Truhlar method were done *without* counterpoise corrections. <sup>b</sup> Extrapolated from MP2/aug-cc-pVDZ and MP2/aug-cc-pVTZ with the method of Truhlar et al.<sup>20,22</sup>

<sup>c</sup> Obtained adding to extrapolation 1 the CCSD(T) correction (the difference between the CCSD(T) and MP2 energies) calculated with the 6-31+G(d) basis set. <sup>d</sup> Experimental value (see ref 18 and references therein).

BSSE reaches −2.05 kcal/mol for the benzene–Na<sup>+</sup> complex and −0.95 kcal/mol for the benzene–H<sub>2</sub>O, and it is very small for the most complete ones, where the BSSE tends to vanish on both systems. This reflects the inherently better description of the latter monomers, needing the basis sets of the interacting partner less for the description of their own electronic density. Therefore, it is strongly advisable to use counterpoise corrections when using less complete basis sets in systems with these types of interactions.

**II. Benchmarking of Density Functionals.** In this section, we assess the performance of the 46 DFT functionals (Table 1) used to study the description of cation– $\pi$  and  $\pi$ –Hbond interactions. Tables 4 and 5 include the electronic interaction energies for both systems, the high-level extrapolated MP2/CBS and CCSD(T)/CBS interaction energies, and the experimental values. These last were available for both systems studied here: −3.44 ± 0.09 kcal/mol for benzene–water (see ref 18 and references therein) and −20.70 ± 1.03 kcal/mol for the Na<sup>+</sup>–benzene system.<sup>62</sup> For the Na<sup>+</sup>–benzene system, we have calculated the ZPE energy at the MP2/6-311++G(d,p) level and subtracted it from the experimental value to get the electronic binding energy. A similar procedure was done by others for the benzene–water system.<sup>18</sup> The difference between the experimental and the extrapolated CCSD(T)/CBS interaction energies was 0.33 and 1.97 kcal/mol for the benzene–water and the Na<sup>+</sup>–benzene systems, respectively.

We have taken the experimental value for the water–benzene system as the reference value for this system, as the accuracy of this value is better than the one we can achieve with the present protocol. In the case of benzene–Na<sup>+</sup>, we have preferred to use the CCSD(T) value as the reference for this study. The experimental value is not very accurate (error bar above 1 kcal/mol) and is shadowed by controversy, with measurements differing by over 7 kcal/mol in recent years.<sup>62,63</sup> We have calculated the whole PEPs for each of the 46 functionals. Globally, the results show a tendency of DFT functionals to overestimate the interaction energies.

In Table 4, we have ranked the functionals according to their absolute difference from the CCSD(T)/CBS value (in the bottom of the table) for the benzene–Na<sup>+</sup> system.

The post-HF methods give very satisfactory results and are very close to the experimental value (−20.70 kcal/mol). The difference between the extrapolation with the Truhlar method

and the aug-cc-pVXZ (X = 2–3) basis sets and the Helgaker method and the aug-cc-pVXZ (X = 3–4) basis sets is small (0.4 kcal/mol). The difference between the CCSD(T) and MP2 energies with the aug-cc-pVTZ is only 0.07 kcal/mol. The difference in the extrapolated values using the Truhlar method with and without diffuse functions is only 0.2 kcal/mol at the MP2 level and 0.4 kcal/mol at the CCSD(T) level, suggesting that the extrapolation without diffuse functions can be seen as a viable alternative for larger systems, at least at the MP2 level.

In general, the DFT results are very good (perhaps excellent), as 20 of the 46 functionals calculate this interaction within chemical accuracy and 33 out of 46 within 2 kcal/mol. This result is particularly positive if we consider the magnitude of the interaction that is being calculated. There is no clear correlation between the amount of HF exchange and the binding energy, contrary to what happens with other properties, like activation energies (e.g., see ref 9), even though there is a tendency for functionals with large fractions of HF exchange to give poorer results (e.g., compare the results of M06-L and M06 with the ones of M06-2X and M06-HF). This may be due to the presence of a metal in the system, as it is well documented that large fractions of HF exchange are detrimental for the description of metals (in particular for transition metals). There is no correlation between functional families and accuracy, even though the hybrid meta functionals give slightly poorer average results. On average, HM functionals give the largest binding energies and GGA functionals give smaller. We also noted that all functionals overestimated the interaction energy.

mPWKCIS, B3PW91, BB95, BLYP, M06, and HCTH results are the most accurate. The very popular B3LYP successfully calculates this interaction within chemical accuracy (error of 0.8 kcal/mol).

Moving on to  $\pi$ –Hbond interactions, we have also ranked the functionals according to their  $|\Delta E_{\text{int}}|$  values (Table 5). We have used the experimental value for the ranking even though the geometry of the computational complex (with an HO bond along the 6-fold axis) is not fully coincident with the absolute minimum (but is relevant in terms of the typical orientation found in biological systems, where the strain of the protein backbone overcomes the very shallow minimum in this flat region of the PES). Comparing the results obtained at the extrapolated MP2/CBS level with the system fully relaxed (−3.66 kcal/mol<sup>20</sup>) and our results at the same level, with the HO bond along the 6-fold symmetry axis (−3.72 kcal/mol), we can see that the difference coming from the different geometries is irrelevant.

The two experimental interaction energies reported (using the ZPE corrections of Feller<sup>64</sup> to obtain  $D_e$  from the experimental  $D_0$ ) are slightly less negative than the extrapolated CCSD(T)/CBS results (with values of  $-3.24 \pm 0.28^{18}$  and  $-3.44 \pm 0.09^{18}$ ). We have adopted the second because it is the more precise one.

Here, we can find out that the HM-GGA functionals give the best results in describing  $\pi$ –Hbond interactions, in particular the ones from the Truhlar group, mostly with high fractions of HF exchange. A similar result was found in an earlier study on the same system but included a much smaller number of density functionals.<sup>18</sup> The most accurate functionals are M06-2X, M05-2X, M06-HF, and M05. Five density functionals have calculated this  $\pi$ –Hbond interaction within chemical accuracy, all with high fractions of HF exchange. This observation may reinforce the hypotheses that the failure of the functionals with high fractions of HF exchange in the description of the Na<sup>+</sup>–benzene

interaction should not be due to an incapacity to account accurately for the interaction itself but instead to a less accurate description of one of the binding partners ( $\text{Na}^+$ ). Twenty-seven density functionals resulted in deviations below 2 kcal/mol. The very popular B3LYP functional ranks 33rd, with a  $\Delta E_{\text{int}}$  of 2.17 kcal/mol. The failure in accounting for dispersive interactions may be one of the reasons for this. Even though the main source for attraction is electrostatic (in the sense of a polarized average electronic density), dispersion forces also contribute to binding, and these are partially unaccounted for by B3LYP. Note that these interactions at equilibrium distances occur in a medium-overlapping density regime, in which the density functional can still account (at least in part) for dispersion, contrary to what happens in longer-range interactions, where the density overlap is much less existent or essentially absent. The results are also in line with other benchmark studies, which show that the HM-GGA functionals with large fractions of HF exchange perform well in the calculation of polar noncovalent interactions.

## CONCLUDING REMARKS

We have performed a basis set benchmarking study, using a total of 13 different basis sets, where we also tested the importance of counterpoise corrections for BSSE. The convergence of the DFT (B3LYP) interaction energy with basis set size was surprisingly fast, with truncation errors (relative to aug-cc-pVQZ) below 0.22 kcal/mol for double- $\zeta$  basis sets with (at least) polarization and diffuse functions on heavy atoms. Even smaller truncation errors were found for larger basis sets, as expected. The 6-311++G(2d,2p) basis set represented the best compromise between accuracy and computational time. The basis set superposition error was particularly large for less complete basis sets (up to 2 kcal/mol in the smaller basis sets) and steadily decreased as the basis set increased, which probably reflects the inherently better description of the latter monomers, needing the basis sets of the interacting partner less for the description of their own electronic density.

Cation- $\pi$  and  $\pi$ -Hbond interactions occur at short/medium range, between a highly polarizable center and a strong dipole/charge, in a region where there is still significant density overlap between the interacting molecules, far from the overlap-free region where dispersion interactions are inherently unaccounted for by DFT. The description of the interactions in this region poses a challenge for DFT, as the density functionals must have a good balance between dispersion, repulsion, and dipolar/electrostatic attraction. In general, the density functionals gave very satisfactory results, with a significant number of predictions within chemical accuracy. In the case of  $\pi$ -Hbond interactions, these mostly belong to the hybrid-meta family and have large fractions of Hartree-Fock exchange. The functionals of the Truhlar group were particularly well suited for this purpose. Beyond their adequacy for the description of intermolecular interactions, they present other advantages such as their good performance in thermochemistry and barrier heights,<sup>9,60</sup> which makes them a very good choice for other studies on biological systems (e.g., chemical/enzymatic reactivity), where many factors must be consistently addressed to have an accurate result.

In the case of cation- $\pi$  interactions, there was not a clear correlation between accuracy and functional sophistication (in terms of its dependence on the density gradients) or percentage of HF exchange. One of the most interesting observations is that

despite the large number of functionals predicting interaction energies within chemical accuracy (five for  $\pi$ -Hbond and 20 for cation- $\pi$  interactions), not a single functional has shown chemical accuracy in both. Moreover, if we calculate the average error for these two interactions, only two density functionals resulted in an average error below 1.0 kcal/mol (M06 and HCTH, with average errors of 0.6 and 0.8 kcal/mol). This epitomizes the limitations that density functionals still present nowadays in terms of the generality of their performance and emphasizes the necessity of a careful choice of the density functional (based on benchmarking studies) before embarking on long and complex electronic structure calculations.

## AUTHOR INFORMATION

### Corresponding Author

\*E-mail: mjrmos@fc.up.pt.

## ACKNOWLEDGMENT

This work has been financed by the program FEDER/COMPETE and by the Fundação para a Ciência e a Tecnologia (Project PTDC/QUI-QUI/102760/2008).

## REFERENCES

- (1) Jiang, Y.; Wu, J.; Zu, J. W.; Lu, Y. X.; Hu, G. X.; Yu, Q. S. *Int. J. Quantum Chem.* **2008**, *108* (7), 1294–1303.
- (2) Dougherty, D. A. *J. Nutr.* **2007**, *137* (6), 1504s–1508s.
- (3) Ruan, C. H.; Rodgers, M. T. *J. Am. Chem. Soc.* **2004**, *126* (44), 14600–14610.
- (4) Liu, T.; Zhu, W. L.; Gu, J. D.; Shen, J. H.; Luo, X. M.; Chen, G.; Puah, C. M.; Silman, I.; Chen, K. X.; Sussman, J. L.; Jiang, H. L. *J. Phys. Chem. A* **2004**, *108* (43), 9400–9405.
- (5) Tarakeswar, P.; Choi, H. S.; Lee, S. J.; Lee, J. Y.; Kim, K. S.; Ha, T. K.; Jang, J. H.; Lee, J. G.; Lee, H. J. *Chem. Phys.* **1999**, *111* (13), 5838–5850.
- (6) Atkins, P. W.; Friedman, R. S. *Molecular quantum mechanics*, 4th ed.; Oxford University Press: Oxford, 2005; pp xiv, 573.
- (7) Ghosh, A. *J. Biol. Inorg. Chem.* **2006**, *11* (6), 671–673.
- (8) Schultz, N. E.; Zhao, Y.; Truhlar, D. G. *J. Phys. Chem. A* **2005**, *109* (49), 11127–11143.
- (9) Zhao, Y.; Truhlar, D. G. *Acc. Chem. Res.* **2008**, *41* (2), 157–167.
- (10) Sousa, S. F.; Fernandes, P. A.; Ramos, M. J. *J. Phys. Chem. A* **2007**, *111* (42), 10439–10452.
- (11) Kim, K. S.; Tarakeswar, P.; Lee, J. Y. *Chem. Rev.* **2000**, *100* (11), 4145–4185.
- (12) Zhao, Y.; Truhlar, D. G. *J. Chem. Theory Comput.* **2005**, *1* (3), 415–432.
- (13) van Mourik, T. *J. Chem. Theory Comput.* **2008**, *4* (10), 1610–1619.
- (14) Peverati, R.; Baldrige, K. K. *J. Chem. Theory Comput.* **2008**, *4* (12), 2030–2048.
- (15) Antony, J.; Grimme, S. *Phys. Chem. Chem. Phys.* **2006**, *8* (45), 5287–5293.
- (16) Jurecka, P.; Cerny, J.; Hobza, P.; Salahub, D. R. *J. Comput. Chem.* **2007**, *28* (2), 555–569.
- (17) Zhao, Y.; Truhlar, D. G. *J. Chem. Theory Comput.* **2007**, *3* (1), 289–300.
- (18) Zhao, Y.; Tishchenko, O.; Truhlar, D. G. *J. Phys. Chem. B* **2005**, *109* (41), 19046–19051.
- (19) Frisch, M. J.; Trucks, G. W.; Schlegel, H. B.; Scuseria, G. E.; et al. *Gaussian 03*, Revision C.02.; Gaussian, Inc.: Wallingford CT, 2004.
- (20) Zhao, Y.; Truhlar, D. G. *J. Phys. Chem. A* **2005**, *109* (30), 6624–6627.



- (21) Tsuzuki, S.; Honda, K.; Uchimaru, T.; Mikami, M.; Tanabe, K. *J. Am. Chem. Soc.* **2000**, *122* (46), 11450–11458.
- (22) Truhlar, D. G. *Chem. Phys. Lett.* **1998**, *294* (1–3), 45–48.
- (23) Halkier, A.; Helgaker, T.; Jorgensen, P.; Klopper, W.; Koch, H.; Olsen, J.; Wilson, A. K. *Chem. Phys. Lett.* **1998**, *286* (3–4), 243–252.
- (24) Karton, A.; Tarnopolsky, A.; Lamere, J. F.; Schatz, G. C.; Martin, J. M. L. *J. Phys. Chem. A* **2008**, *112* (50), 12868–12886.
- (25) Silva, M. R.; Schreiber, M.; Sauer, S. P. A.; Thiel, W. *J. Chem. Phys.* **2008**, *129* (10).
- (26) Zhao, Y.; Truhlar, D. G. *J. Phys. Chem. C* **2008**, *112* (17), 6860–6868.
- (27) Settergren, N. M.; Buhlmann, P.; Amin, E. A. *THEOCHEM* **2008**, *861* (1–3), 68–73.
- (28) Santra, B.; Michaelides, A.; Scheffler, M. *J. Chem. Phys.* **2007**, *127* (18), -.
- (29) Amin, E. A.; Truhlar, D. G. *J. Chem. Theory Comput.* **2008**, *4* (1), 75–85.
- (30) Sousa, S. F.; Fernandes, P. A.; Ramos, M. J. *J. Phys. Chem. B* **2007**, *111* (30), 9146–9152.
- (31) Lee, C. T.; Yang, W. T.; Parr, R. G. *Phys. Rev. B* **1988**, *37* (2), 785–789.
- (32) Becke, A. D. *Phys. Rev. A* **1988**, *38* (6), 3098–3100.
- (33) Tao, J. M.; Perdew, J. P.; Staroverov, V. N.; Scuseria, G. E. *Phys. Rev. Lett.* **2003**, *91* (14).
- (34) Vosko, S. H.; Wilk, L.; Nusair, M. *Can. J. Phys.* **1980**, *58* (8), 1200–1211.
- (35) Perdew, J. P. *Phys. Rev. B* **1986**, *33* (12), 8822–8824.
- (36) Perdew, J. P. Unified Theory of Exchange and Correlation Beyond the Local Density Approximation. In *Electronic Structure of Solids*; Zieche, P., Eschrig, H., Eds.; Akademie: Berlin, Germany, **1991**.
- (37) Becke, A. D. *J. Chem. Phys.* **1996**, *104* (3), 1040–1046.
- (38) Van Voorhis, T.; Scuseria, G. E. *J. Chem. Phys.* **1998**, *109* (2), 400–410.
- (39) Perdew, J. P.; Burke, K.; Ernzerhof, M. *Phys. Rev. Lett.* **1996**, *77* (18), 3865–3868.
- (40) Gill, P. M. W. *Mol. Phys.* **1996**, *89* (2), 433–445.
- (41) Krieger, J. B.; Chen, J. Q.; Iafrate, G. J.; Savin, A. *Electron. Correl. Mater. Prop.* **1999**, 463–477.
- (42) Hamprecht, F. A.; Cohen, A. J.; Tozer, D. J.; Handy, N. C. *J. Chem. Phys.* **1998**, *109* (15), 6264–6271.
- (43) Zhao, Y.; Truhlar, D. G. *J. Chem. Phys.* **2006**, *125* (19), -.
- (44) Handy, N. C.; Cohen, A. J. *Mol. Phys.* **2001**, *99* (5), 403–412.
- (45) Xu, X.; Goddard, W. A. *Proc. Natl. Acad. Sci. U.S.A.* **2004**, *101* (9), 2673–2677.
- (46) Perdew, J. P.; Wang, Y. *Phys. Rev. B* **1992**, *45* (23), 13244–13249.
- (47) Becke, A. D. *J. Chem. Phys.* **1993**, *98* (7), 5648–5652.
- (48) Zhao, Y.; Truhlar, D. G. *J. Phys. Chem. A* **2004**, *108* (33), 6908–6918.
- (49) Adamo, C.; Barone, V. *J. Chem. Phys.* **1998**, *108* (2), 664–675.
- (50) Zhao, Y.; Gonzalez-Garcia, N.; Truhlar, D. G. *J. Phys. Chem. A* **2005**, *109* (9), 2012–2018.
- (51) Zhao, Y.; Lynch, B. J.; Truhlar, D. G. *Phys. Chem. Chem. Phys.* **2005**, *7* (1), 43–52.
- (52) Schmider, H. L.; Becke, A. D. *J. Chem. Phys.* **1998**, *108* (23), 9624–9631.
- (53) Becke, A. D. *J. Chem. Phys.* **1997**, *107* (20), 8554–8560.
- (54) Zhao, Y.; Schultz, N. E.; Truhlar, D. G. *J. Chem. Phys.* **2005**, *123* (16), -.
- (55) Lynch, B. J.; Fast, P. L.; Harris, M.; Truhlar, D. G. *J. Phys. Chem. A* **2000**, *104* (21), 4811–4815.
- (56) Zhao, Y.; Schultz, N. E.; Truhlar, D. G. *J. Chem. Theory Comput.* **2006**, *2* (2), 364–382.
- (57) Wilson, P. J.; Bradley, T. J.; Tozer, D. J. *J. Chem. Phys.* **2001**, *115* (20), 9233–9242.
- (58) Zhao, Y.; Truhlar, D. G. *J. Phys. Chem. A* **2006**, *110* (49), 13126–13130.
- (59) Hoe, W. M.; Cohen, A. J.; Handy, N. C. *Chem. Phys. Lett.* **2001**, *341* (3–4), 319–328.
- (60) Zhao, Y.; Truhlar, D. G. *Theor. Chem. Acc.* **2008**, *120* (1–3), 215–241.
- (61) Frisch, M. J.; Trucks, G. W.; Schlegel, H. B.; Scuseria, G. E.; et al. *Gaussian 09*, Revision A.02.; Gaussian, Inc.: Wallingford, CT, 2009.
- (62) Armentrout, P. B.; Rodgers, M. T. *J. Phys. Chem. A* **2000**, *104* (11), 2238–2247.
- (63) Ma, J. C.; Dougherty, D. A. *Chem. Rev.* **1997**, *97* (5), 1303–1324.
- (64) Feller, D. *J. Phys. Chem. A* **1999**, *103* (38), 7558–7561.